

Supplementary Materials for A “cation-anion regulation” synergistic anode host for dendrite-free lithium metal batteries

Weidong Zhang, Houlong L. Zhuang, Lei Fan, Lina Gao, Yingying Lu

Published 23 February 2018, *Sci. Adv.* **4**, ear4410 (2018)

DOI: 10.1126/sciadv.aar4410

The PDF file includes:

- fig. S1. Sketch of the structures of PP separator and Li atom after geometry optimizations.
- fig. S2. Images of q-PET nonwoven fabric.
- fig. S3. SEM and elemental mapping images showing the homogenous distribution of C, N, and O in the q-PET fiber.
- fig. S4. EDX spectrum under SEM mode.
- fig. S5. Cycling performances of Li/Cu cells.
- fig. S6. Digital picture of q-PET interlayer after 30 cycles.
- fig. S7. Effectiveness of lithiophilic effect only.
- fig. S8. SEM images of Li deposition on q-PET fiber–modified electrodes after 10 cycles.
- fig. S9. Galvanostatic cycling performance of symmetrical cells.
- fig. S10. Galvanostatic cycling performance of symmetrical cells at 5 mA cm⁻² with high areal capacities of 2, 5, or 10 mA·hour cm⁻².
- fig. S11. Charge-discharge profiles of the Li/LFP cells at different cycles.
- fig. S12. Voltage profiles of Li/LFP and Li/LTO half cells with or without q-PET (first cycle).
- table S1. Binding energies using DFT calculations.
- table S2. Elemental analysis (Dumas combustion).
- table S3. Li CE of q-PET–modified cells compared with other state-of-the-art modifications.
- Legends for movies S1 and S2
- References (38–45)

Other Supplementary Material for this manuscript includes the following:

(available at advances.sciencemag.org/cgi/content/full/4/2/eaar4410/DC1)

- movie S1 (.mp4 format). Shape of a droplet (ether-based electrolyte) on the bare lithium foil.
- movie S2 (.mp4 format). Spreading behavior of a droplet (ether-based electrolyte) on the q-PET/Li composite anode.

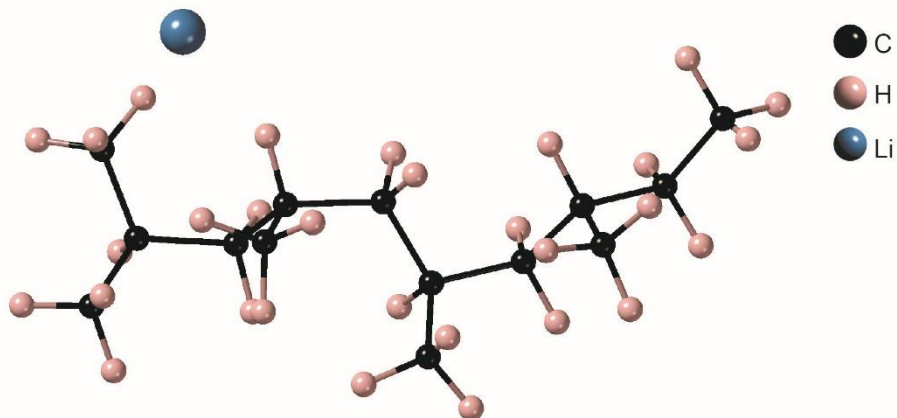


fig. S1. Sketch of the structures of PP separator and Li atom after geometry optimizations.

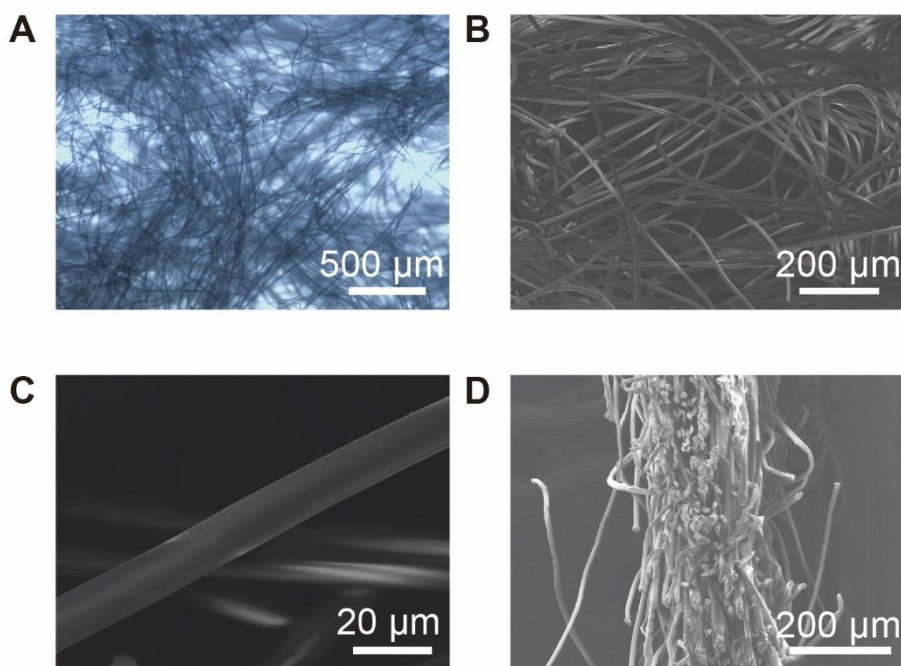


fig. S2. Images of q-PET nonwoven fabric. (A) The optical microscopy image of q-PET nonwoven fabric. (B) SEM images of q-PET nonwoven fabric. (C) SEM images of individual q-PET fiber. (D) The cross-sectional SEM image of q-PET nonwoven fabric.

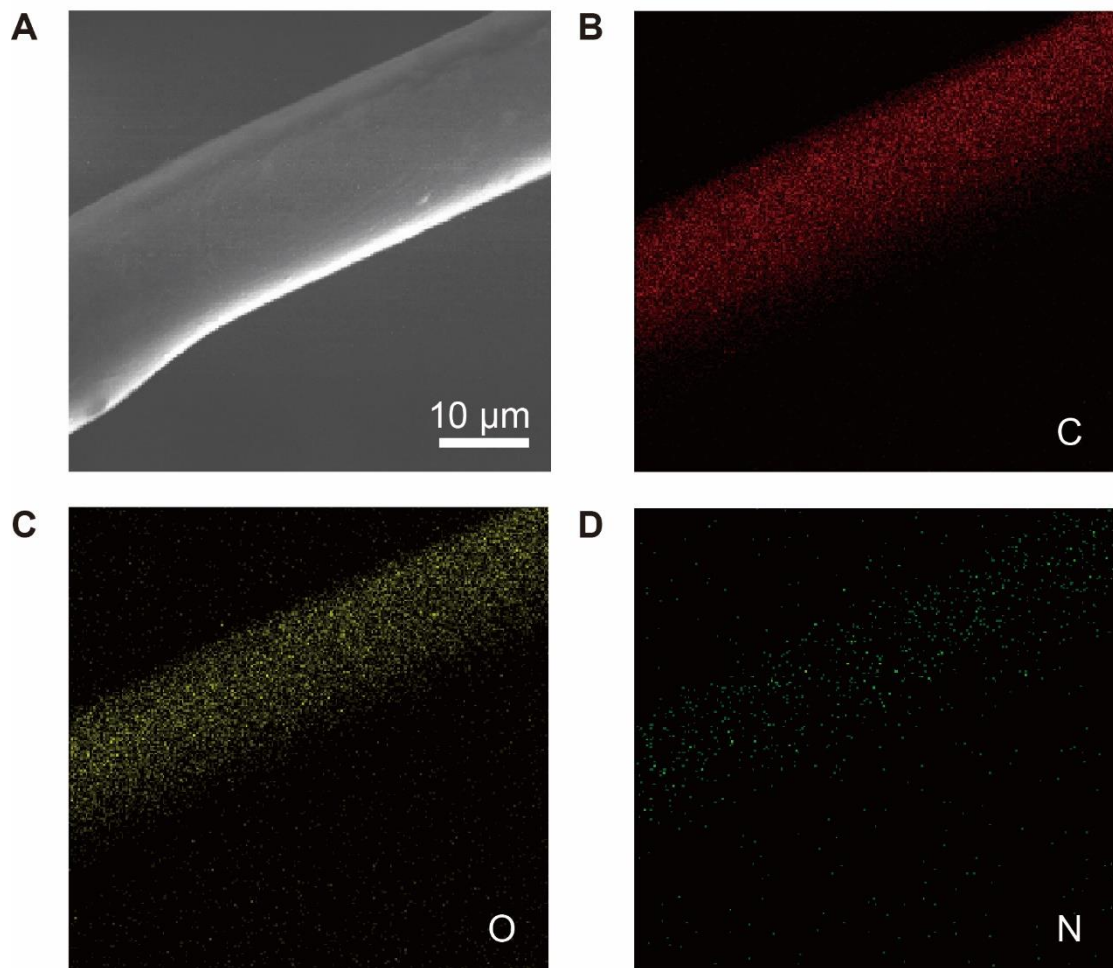


fig. S3. SEM and elemental mapping images showing the homogenous distribution of C, N, and O in the q-PET fiber.

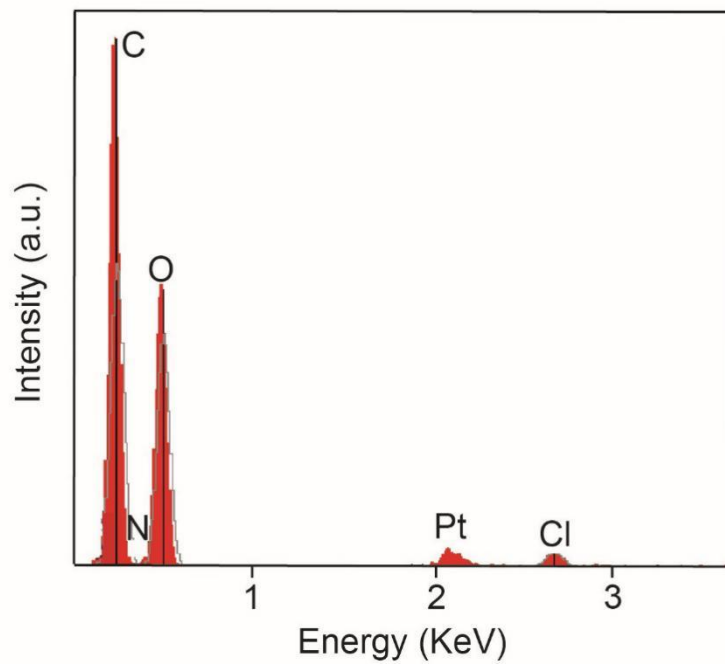


fig. S4. EDX spectrum under SEM mode.

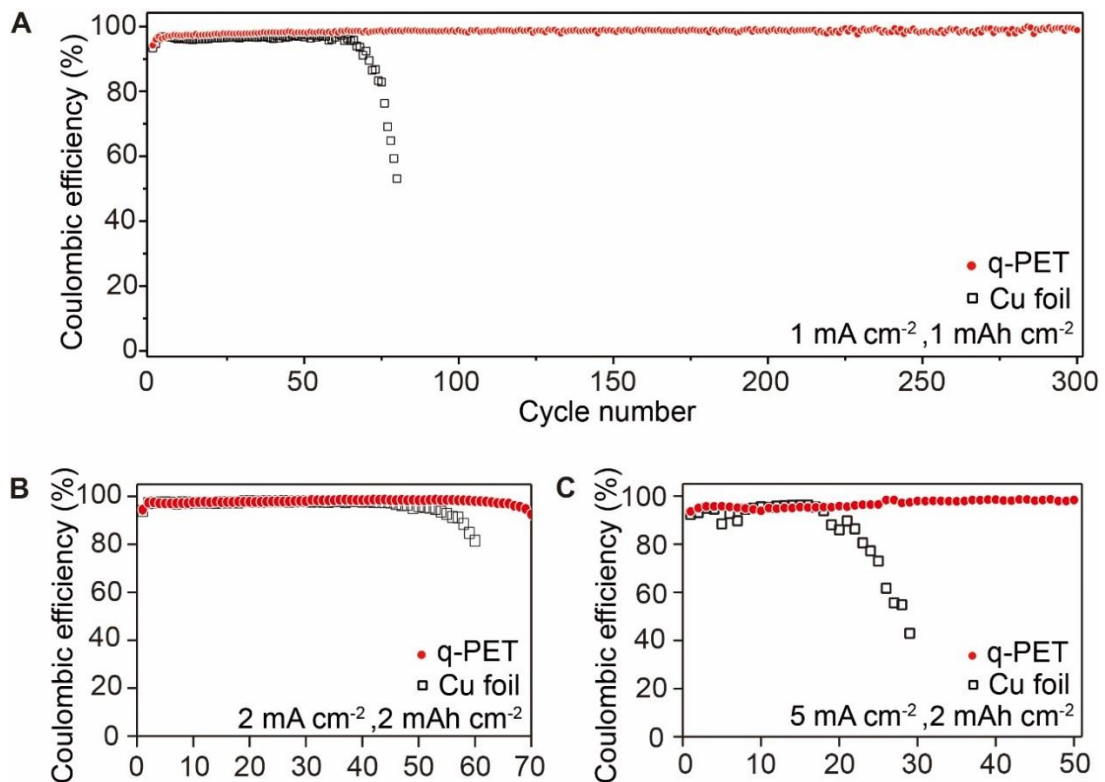


fig. S5. Cycling performances of Li/Cu cells. (A) Long-term electrochemical performance of Li/Cu cells at 1 mA cm^{-2} with a capacity of 1 mAh cm^{-2} . (B and C) Comparison of Coulombic efficiency of Cu foil with and without q-PET fabric at various current rates of (B) 2 mA cm^{-2} and (C) 5.0 mA cm^{-2} with the same areal capacity of 2.0 mAh cm^{-2} .

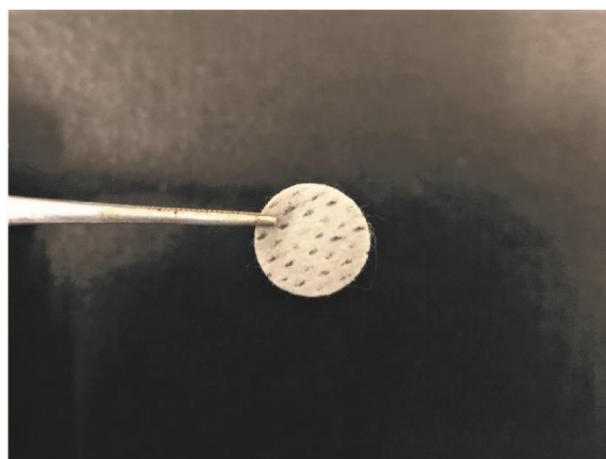


fig. S6. Digital picture of q-PET interlayer after 30 cycles.

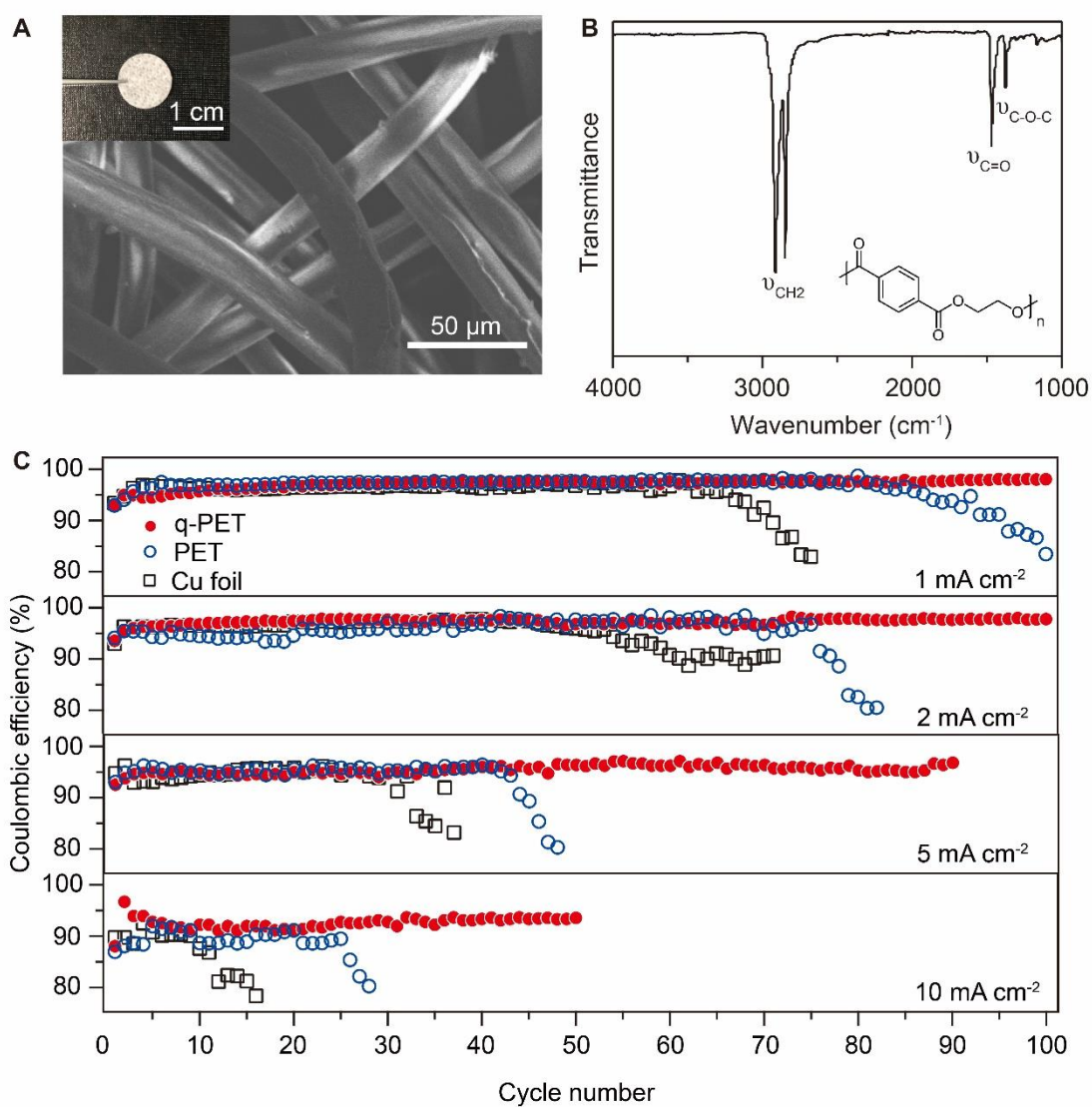


fig. S7. Effectiveness of lithiophilic effect only. (A) SEM image of poly (ethylene terephthalate) (PET) fiber network. The inset shows the digital picture of PET fabric.

(B) FTIR spectrum of PET. (C) Lithium Coulombic efficiencies of cells with bare Cu foil, with PET (“lithiophilic effect only”), or with q-PET (“lithiophilic-anionphilic synergistic effect”) at various current densities with the same areal capacity of 1.0 mAh cm^{-2} .

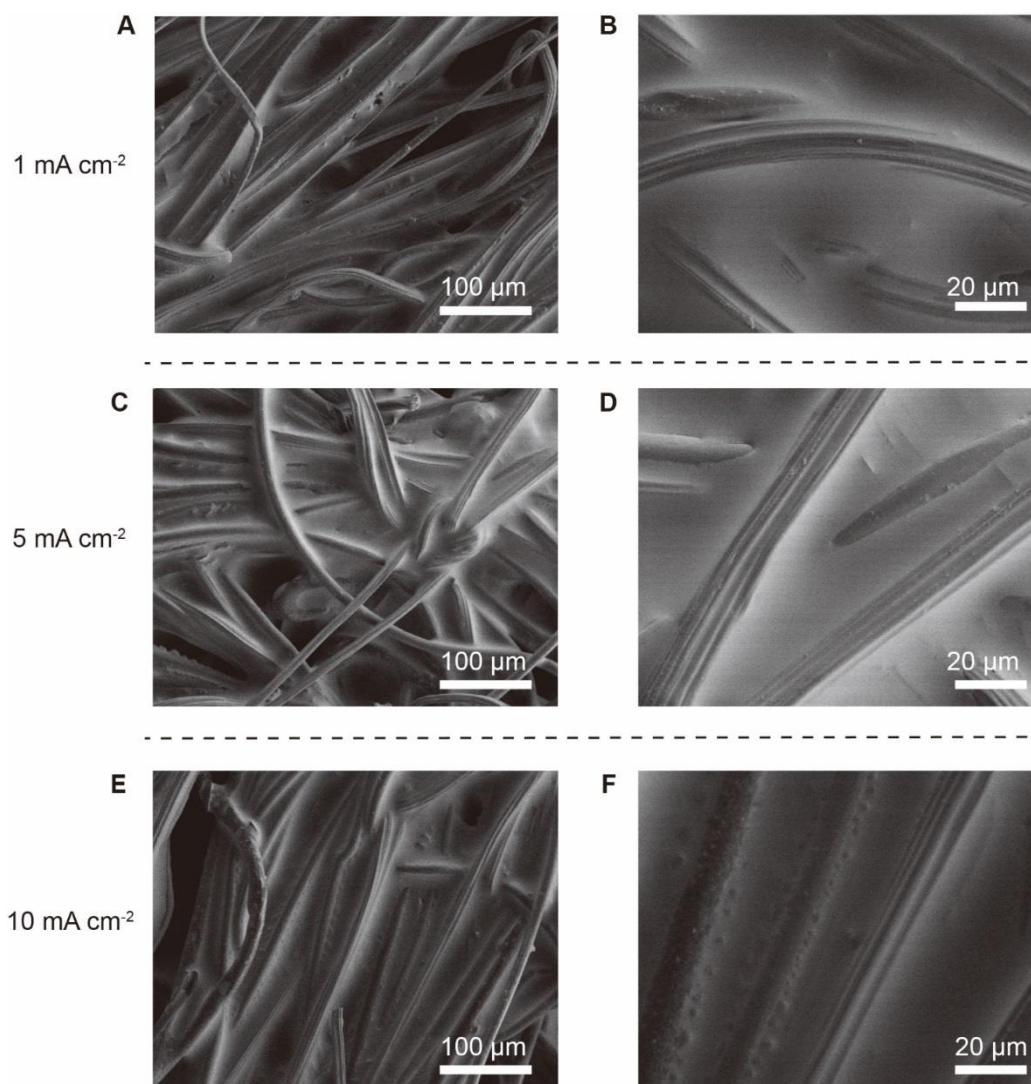


fig. S8. SEM images of Li deposition on q-PET fiber-modified electrodes after 10 cycles.

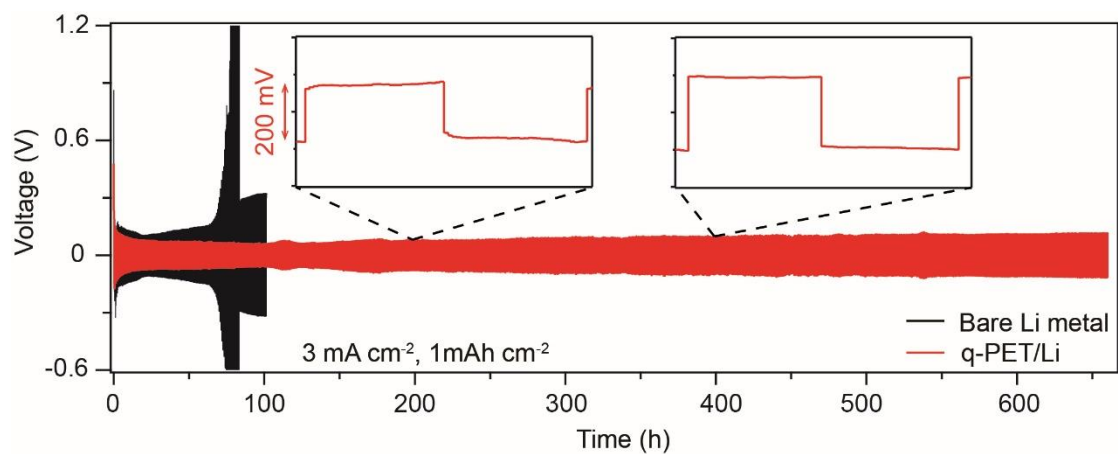


fig. S9. Galvanostatic cycling performance of symmetrical cells.

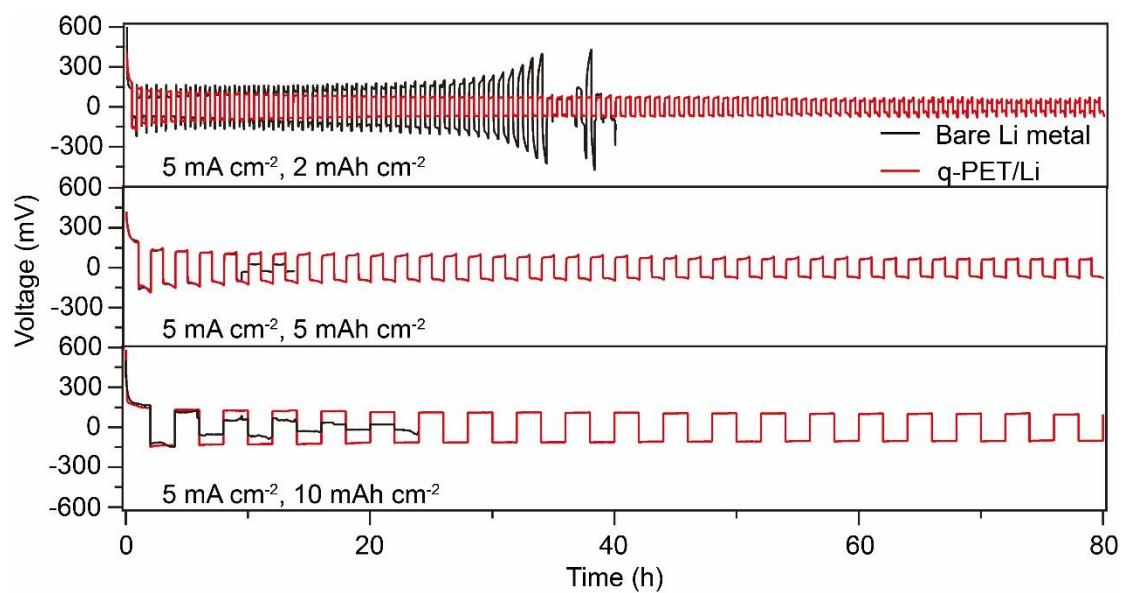


fig. S10. Galvanostatic cycling performance of symmetrical cells at 5 mA cm^{-2} with high areal capacities of 2, 5, or $10 \text{ mA}\cdot\text{hour cm}^{-2}$.

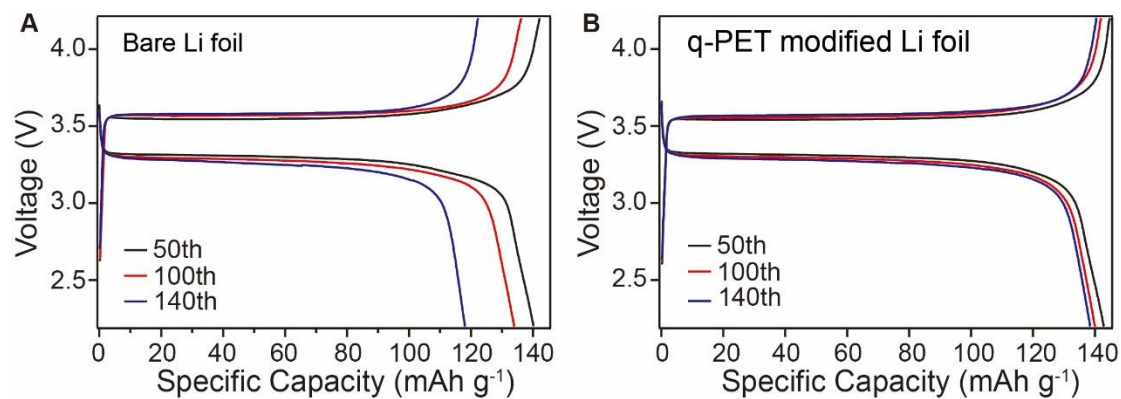


fig. S11. Charge-discharge profiles of the Li/LFP cells at different cycles. (A) Charge-discharge profiles of the Li/LiFePO₄ cells at 0.5 C using bare Li foil, and **(B)** using q-PET modified Li foil.

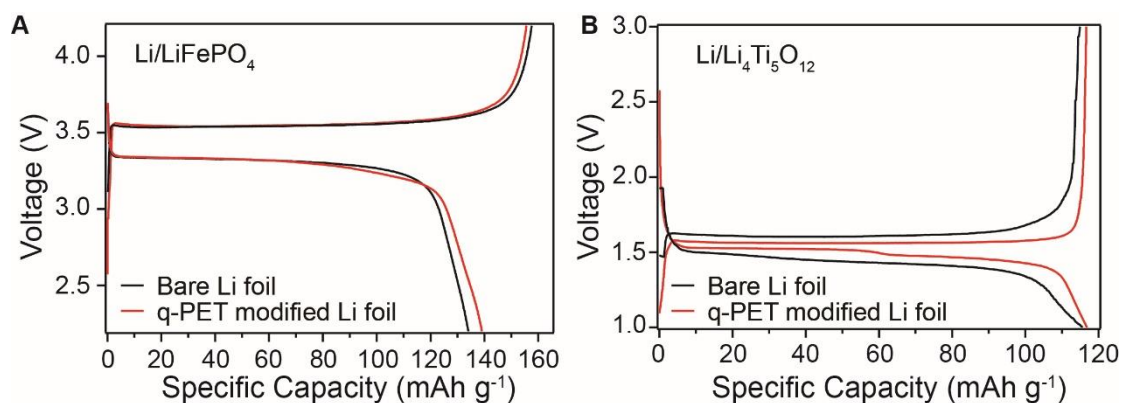


fig. S12. Voltage profiles of Li/LFP and Li/LTO half cells with or without q-PET (first cycle).

table S1. Binding energies using DFT calculations.

Materials	Binding energy E_b
q-PET with TFSI anion	3.93 eV
q-PET with Li-ion	0.69 eV
Polypropylene separator with Li-ion	-0.35 eV

table S2. Elemental analysis (Dumas combustion).

Sample Name	N content (wt%)	C content (wt%)	H content (wt%)
q-PET fiber	0.52	58.57	7.72

table S3. Li CE of q-PET–modified cells compared with other state-of-the-art modifications.

Current / Capacity (mAh cm ⁻² / mAh m ⁻²)	CE / Lifespan (%/cycles)	Modifications	ref
0.5 / 0.5	98 / 90	glass fiber	(18)
	98.7 / 120	LiF protected	(38)
0.5 / 1.0	97.5 / 100	3D Cu current collector/Li	(39)
	99 / 100	LiF artificial SEI	(26)
	97.6 / 120	silly putty	(40)
1.0 / 0.5	97 / 67	glass fiber	(18)
	97.6 / 240	polyimide coating	(41)
1.0 / 1.0	97.0 / 120	silly putty	(40)
	97.9 / 120	polymer nanofiber	(17)
	98 / 200	nirtrogen doped graphene	(42)
	97.4 / 100	Cu ₃ N artificial SEI	(43)
	95 / 120	In(TFSI) ₃ additive	(8)
	98.2 / 100	PDMS coating	(44)
	98 / 300	this work	
2.0 / 0.5	96 / 63	glass fiber	(18)
	96.5 / 60	β-PVDF coating	(45)
	92.9 / 150	polyimide coating	(41)
2.0 / 1.0	93 / 60	PDMS coating	(44)

	96 / 100	nirtrogen doped graphene	(42)
	97 / 100	this work	
5.0 / 0.5	93 / 48	glass fiber	(18)
	92.5 / 60	β -PVDF coating	(45)
5.0 / 1.0	95 / 90	this work	
10 / 0.5	91 / 40	glass fiber	(18)
10 / 1.0	93 / 50	this work	

movie S1. Shape of a droplet (ether-based electrolyte) on the bare lithium foil.
movie S2. Spreading behavior of a droplet (ether-based electrolyte) on the q-PET/Li composite anode.